Research Square

Preprints are preliminary reports that have not undergone peer review.
They should not be considered conclusive, used to inform clinical practice,
or referenced by the media as validated information.

Improving the wear resistance of cutting tools during steels machining

Gislain Anicet Zebaze Ndjapou

ndjaze@gmail.com

Volgograd State Technical University: Volgogradskij gosudarstvennyj tehniceskij universitet
https://orcid.org/0009-0004-1821-2965

Julius L Tchigirinsky

Volgograd State Technical University: Volgogradskij gosudarstvennyj tehniceskij universitet

Research Article

Keywords: cutting tool, physical deposition, chemical deposition, tungsten carbide WC-Co, thermal Conductivity, wear resistant coatings, tool wear, diffusion coating, specific heat capacity

Posted Date: November 27th, 2026

DOI: https://doi.org/10.21203/rs.3.rs-11749388/v1

License: This work is licensed under a Creative Commons Attribution 4.0 International License.
Read Full License

Original article

Improving the wear resistance of cutting tools during steels machining

Gislain Anicet Zebaze Ndjapou[1], Julius L. Tchigirinsky[1]*

[1]**Volgograd State Technical University, Department of Mechanical Engineering, Volgograd, Russian Federation**

*Corresponding author: Gislain Anicet Zebaze Ndjapou

E-mail: ndjaze@gmail.com

ORCID: 0009-0004-1821-2965

Abstract

This article examines tungsten carbide (WC-Co) inserts coated by physical vapor deposition (PVD - AlTiN) and chemical vapor deposition (CVD - TiCN + Al_2O_3) as two major solutions for improving the wear resistance of carbide cutting tools. One of the main technical and economic challenges of modern machining lies in improving the durability of cutting tools when machining corrosion resistant stainless steels. By analyzing cutting forces (F_C), interface temperature (θ_i), and monitoring wear kinetics (V_B), we evaluate the performance of these coatings to optimize tool life under severe cutting conditions. The results demonstrate that while the PVD coating performs well during the first few minutes by limiting work hardening, the alumina thermal barrier of the CVD coating extends the overall tool life by nearly 35% under stationary and severe cutting conditions. The breakdown of the cobalt bond between the tungsten carbide grains leads to fractures on the surface of the cutting tool, which causes fractures and mechanical detachment of the grains from the cutting edge surface, corresponding to crack wear. Combined technologies for modifying the cutting tool surface are of major practical interest.

Keywords: *cutting tool, physical deposition, chemical deposition, tungsten carbide WC-Co*, *thermal Conductivity, wear resistant coatings, tool wear, diffusion coating, specific heat capacity*

1. Introduction

In the high-precision machining industry, the durability of cutting tools when machining difficult-to-machine materials represents a major technical and economic challenge [1-2]. Austenitic steel 12X18H10T (AISI 321 equivalent), containing approximately 18% chromium, 10% nickel, and stabilized with titanium, is known for its low thermal conductivity, which concentrates heat on the cutting edge; its high work hardening, which increases the required shear forces; and its strong chemical affinity with binders, causing premature wear of cutting tools [3-4].

In today's competitive industrial environment, machining efficiency is measured by cutting speed. Tool life, process stability, surface finish, and part cost are all key factors in improving overall productivity. One of the most effective ways to optimize machining performance is through the use of high-performance cutting tool coatings [5-7]. The tool represents the weakest link in production processes, as its wear is a major cause of decreased production quality and increased production costs [8].

Acting as a thermal and chemical barrier, physical vapor deposition (PVD) and chemical vapor deposition (CVD) surface coatings enable mechanical engineers to optimize

tool life while increasing production in demanding applications [9-10]. Uncoated cutting tools are rarely reliable in modern production due to their poor resistance to wear, heat, and chemical interactions with the workpiece. The advanced coatings presented in this article form a protective and functional layer between the tool substrate and the cutting zone, thereby reducing friction, resistance to wear mechanisms such as abrasion, adhesion, diffusion, and oxidation, and improving thermal stability. Coating technologies are thus designed to work on a wide range of materials, including carbon steels, stainless steels, cast irons, superalloys, and hardened materials, enabling consistent results in general and high-precision machining [11].

Although advanced coatings can increase the initial cost of a cutting tool, their impact on the overall manufacturing economics is significant. Extended tool life reduces tool change frequency and machine downtime, while the ability to operate at higher speeds and feed rates increases material removal rates and shortens cycle times [12]. With machining evolving towards greater efficiency, tighter tolerances, and increased automation, advanced PVD and CVD coatings are no longer an option but a necessity for improving metal machining. This study quantifies and models the performance of these two technologies on 12X18H10T austenitic steel.

2.Materials and Methods

External turning tests were performed on a high-speed rigid CNC turning machine. The test specimen was a cylindrical 12X18H10T steel bar (AISI 321 equivalent) with dimensions of Ø60 × 120 mm, the chemical composition of which is detailed in Table 1. A coated tungsten carbide cutting tool, containing 8 wt% cobalt (Co) and having a WC grain size of 0.8 μm, was used. This tool was first coated with TiAlN (titanium-aluminum nitride) by physical vapor deposition (PVD), and then with TiCN + Al_2O_3 (alumina) by chemical vapor deposition (CVD). The geometric characteristics were as follows: rake angle γ = 12°, clearance Angle α = 7°, angle to the plane φ = 45°, and nose radius $r_{bec} = 0{,}4\ mm$. The cutting conditions were standardized to: cutting speed $V = 140\ m/min$, feed rate $f = 0{,}2\ mm/rev$, and depth of cut $a_p = 1{,}5\ mm$. The experimental system, consisting of a numerically controlled (CNC) lathe, an induction heating system, a TiAlN-coated carbide cutting tool, 12X18H10T steel, temperature sensors (thermocouples), a data logger, a data acquisition and processing unit, and a cooling system, is shown in Figure 1.

Table 1 Chemical composition of steels (in wt.%, balance Fe).

Grade steel	C	Cr	Ni	Mn	Si	Ti	P	S	Cu
12X18H10T	0,12	18,00	10,00	1,50	0,60	0,50	0,035	0,020	0,30

In accordance with existing literature [13-14], to ensure thermal stability and chemical resistance, the TiAlN coating forms an in-situ protective alumina (Al_2O_3) layer under the effect of the cutting heat. This Al_2O_3 layer blocks atomic diffusion between the chip and the tool at temperatures above 900℃. The characteristics of the two tools are presented in Table 2. Dynamic forces were measured using a triaxial piezoelectric dynamometer connected to a high-frequency data acquisition system. The wear (V_B) was measured at regular intervals using the computer system connected to the experimental setup, and the morphology of the worn edge was characterized by scanning electron microscopy (SEM). This study was conducted to develop durable dry machining and to evaluate the efficiency of coated carbide tools.

Table 2 Characteristics of PVD and CVD tools.

Technical Parameter	PVD (TiAlN) Tool	CVD (TiCN + Al_2O_3) Tool
Deposition Temperature	300 ℃ – 500 ℃	850 ℃ – 1050 ℃
Coating Thickness	$2 - 4\ \mu m$	$8 - 20\ \mu m$
Edge Radius	$r_\beta \approx 5 - 15\ \mu m$	$r_\beta \approx 30 - 50\ \mu m$
Microhardness	3000 – 3300 HV	2800 HV for TiCN/ 2200 HV for Al_2O_3
Thermal Conductivity	$11\ W/(m \cdot K)$	$5\ W/(m \cdot K)$
Oxidation Resistance Temp.	800°C – 900°C	1100°C – 1200°C

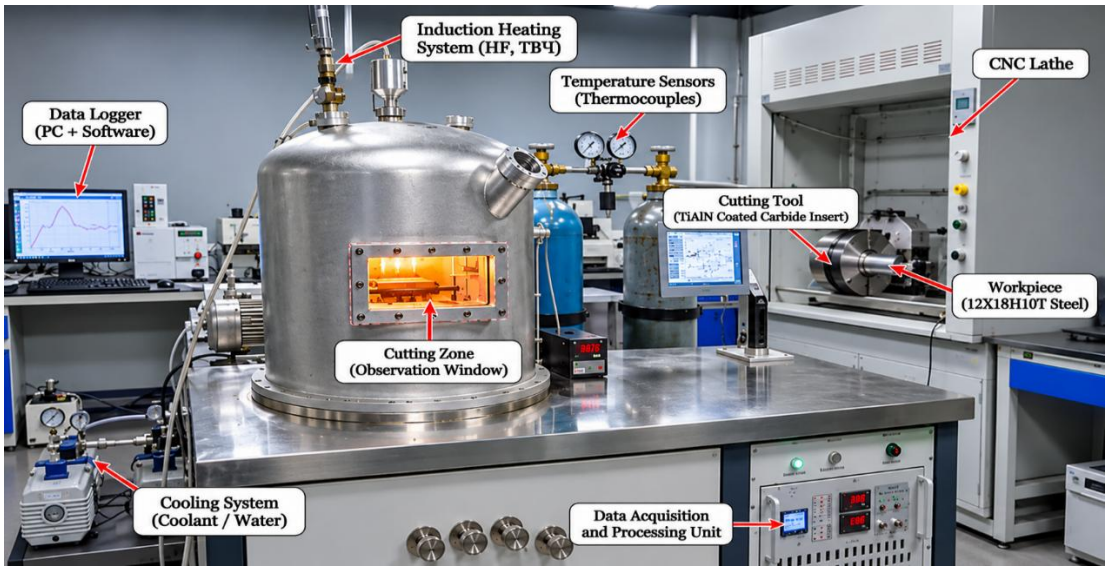


Figure 1 Experimental setup for the turning of austenitic stainless steel 12X18H10T.

3. Results and Discussion

The thermomechanical behavior and degradation kinetics of coated carbide inserts during the turning of titanium-stabilized austenitic steel 12X18H10T can be interpreted in detail by the interaction of coating properties, process variables, and the workpiece metallurgy. Temperature increases modify the heat flow, resulting in a nonlinear variation in the thermal

conductivity and heat capacity of the steel (see Figure 2). The transition from one crystalline structure to another (transformation of ferrite/pearlite to austenite by heating) creates marked discontinuities or peaks in the evolution of thermophysical properties [15-17]. Variations in thermal diffusivity modify the plastic behavior of the steel; the chip deforms more easily without adhering to the tool, thus reducing tool wear.

Table 3 Thermophysical properties of Steel 12X18H10T as a function of temperature.

T (°C)	λ (W/(m·K))	C_p (J/(kg·K))	ρ_e (nΩ·m)	α (10^{-6} 1/°C)	E (10^{-5}·MPa)
20	15	462	725	16,6	1,98
100	16	496	792	17,0	1,94
200	18	517	861	17,2	1,89
300	19	538	920	17,5	1,81
400	21	550	976	17,9	1,74
500	23	563	1028	18,2	1,66
600	25	575	1075	18,6	1,57
700	27	596	1115	18,9	1,47
800	26	598	1150	19,3	1,24

The thermophysical properties detailed in Tables 3 such as λ (thermal conductivity), C_p (specific heat capacity of the material), ρ_e (electrical resistivity), α (coefficient of linear thermal expansion), E (modulus of elasticity), and T (temperature) - all depend on temperature due to the non-linear nature of the turning process.

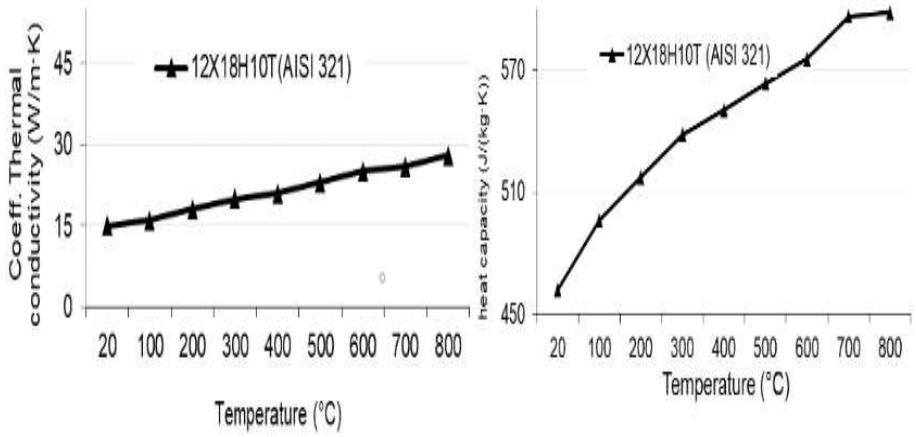


Figure 2 Thermophysical properties of steel as a function of temperature.

Due to the low thermal conductivity ($\lambda \approx 15\, W/(m \cdot K)$) and high specific heat capacity ($C_p \approx 500\, J/kg \cdot K$) of 12X18H10T steel, most of the plastic deformation energy is converted into localized thermal energy. The total heat generated in the cutting zone (Q_T) during turning depends on the cutting speed and force:

$$Q_T = F_C \cdot V \quad (1)$$

Using Cook's thermo-analytical model [18], the average temperature at the tool-chip interface (θ_i) can be expressed as follows:

$$\theta_i = 0.4 \cdot \frac{K_S}{\rho \cdot C_p} \cdot \left(\frac{V \cdot f}{\alpha}\right)^{0.333} \quad (2)$$

Where :

- K_s is the specific cutting pressure of the 12X18H10T steel (≈ 2200 MPa due to its high shear resistance).
- ρ is the density ($7920\ kg/m^3$).
- α is the thermal diffusivity of the steel, calculated as $\alpha = \frac{\lambda}{\rho \cdot C_p} \approx 3.79 \times 10^{-6} m^2/s$.

Substituting our operating values ($V = 140\ m/\min\ and\ f = 0{,}2\ mm/rev$), the theoretical model yields an extreme interface temperature of $\theta_i \approx 935$°C. At this temperature, the tool wear kinetics are controlled by the physical properties of the coated inserts [16]. Since the thermal conductivity of alumina is extremely low ($\lambda_{Al_2O_3} \approx 5\ W/(m \cdot K)$ hot) during CVD coating, it acts as a thermal shield, forcing approximately 85% of the heat to dissipate directly into the chip. The carbide (WC-Co) substrate thus retains its intrinsic hardness. Although AlTiN undergoes surface oxylysis under the influence of heat to form a thin passive alumina layer, its overall conductivity remains higher ($\lambda_{AlTiN} \approx 11\ W/(m \cdot K)$) during PVD coating. At a cutting speed $V = 140 m/min$, the heat flux penetrates the coated layer and thermally softens the carbide substrate. The values of the mechanical forces, interface temperatures, and wear propagation obtained after 15 minutes of turning are summarized in Table 4. The critical wear criterion was set at $V_B = 0.3\ mm$.

Table 4 Thermomechanical and kinetic data on tool wear.

Cutting Time t (min)	**Tangential Force F_C (N)**	**Interface Temperature θ_i (°C)**	**Wear V_B - PVD AlTiN (mm)**	**Wear V_B - CVD TiCN+Al_2O_3 (mm)**
0 **(New Tool)**	1150	780	0.00	0.00
1	1180	810	0.05	0.08
3	1210	845	0.11	0.13
5	1260	890	0.18	0.17
8	1340	925	0.26	0.21
10	1410	935	**0.32** (Critical Limit)	0.24
12	1490	955	0.41 (Failure)	0.27
14	1580	980	-	**0.31** (Critical Limit)
15	1650	1010	-	0.36 (Failure)

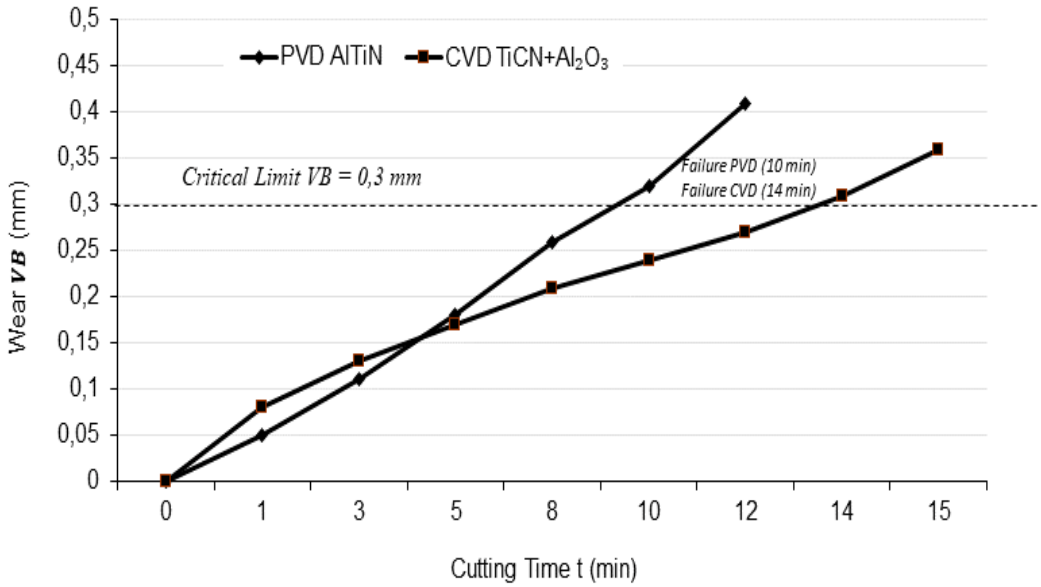


Figure 3 Wear evolution curves V_B as a function of time.

The tribological response of the two tools (PVD AlTiN and CVD TiCN+Al_2O_3) is strongly influenced by the metallurgy of the titanium-stabilized 12X18H10T steel. The kinetics reveal a clear inflection point in performance at $t = 5\ min$. The PVD tool exhibits less wear ($V_B = 0{,}11\ mm$ versus $0{,}13\ mm$ for CVD) over a time interval of $[0 - 3\ ]min$. The PVD process produces a much sharper geometric edge (absence of the rounding inherent in CVD). This reduces initial friction and limits work hardening of the workpiece. Beyond 5 minutes, the PVD tool undergoes accelerated wear due to thermal degradation of the substrate. It crosses the critical wear threshold ($V_B = 0{,}3\ mm$) at $t = 10\ min$. Conversely, the CVD tool stabilizes its wear thanks to the thermal insulation of the alumina layer, crossing the critical limit $t = 14\ min$.

The surface morphology of the workpiece after machining is shown in Figure 4. Figures 4.a) and 4.b) reveal a heavily damaged machined surface, exhibiting numerous scratches and tool pits, indicative of significant tool vibration during cutting. This results in an extremely unstable cutting process, accompanied by adhesion defects due to material buildup. In the absence of a heat source during machining, significant friction and extrusion occur between the tool and the workpiece surface, leading to substantial material removal. Consequently, tool wear is rapid, and the surface quality deteriorates quickly. The more regular appearance of the machining marks observed in Figures 4.c) and 4.b) indicates a potential improvement in surface finish due to induction heating. The surface is relatively smooth and flat, the machining marks are minimal, and the overall morphology shows no apparent defects. This change is due to the fact that the additional energy input in the form of induction causes a

rapid increase in temperature in the cutting zone, a decrease in resistance to plastic deformation, and a modification of the tool-chip contact conditions, thus facilitating material removal and reducing mechanical stress on the tool as well as friction between the workpiece and the tool.

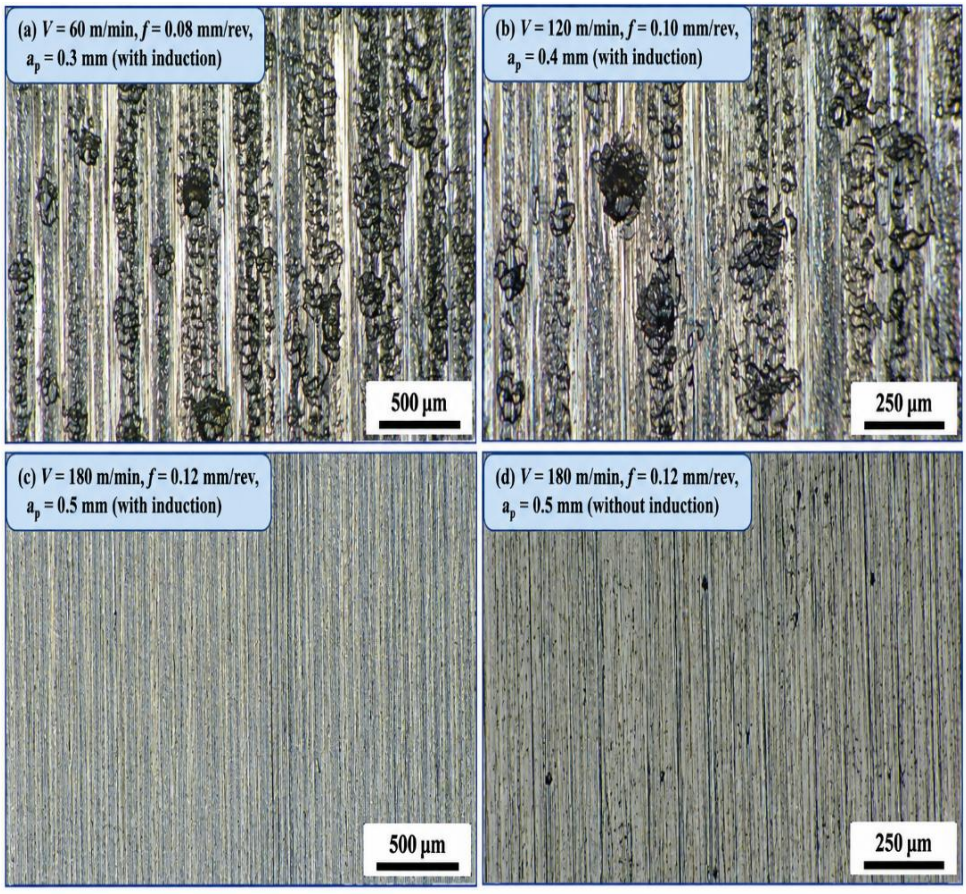


Figure 4 Surface morphology of machined 12X18H10T steel.

Tool wear is one of the key factors influencing machining costs and surface quality when turning 12X18H10T steel. The observed wear mechanism is illustrated in Figure 5. Scanning electron microscopy (SEM) analysis of the tools after 10 minutes of machining reveals distinct tribological behaviors. First, on the PVD (AlTiN) tool, the cutting edge undergoes cyclic adhesion wear. The 12X18H10T austenitic steel locally welds to the tool surface under pressure. During chip evacuation, fragments of the AlTiN coating flake off, directly exposing the tungsten carbide to abrasion by titanium inclusions in the matrix. Finally, on the CVD (TiCN+Al_2O_3) tool, the cutting edge exhibits smooth and uniform micro-abrasion wear. The chemical inertness of the Al_2O_3 outer phase eliminates the affinity for nickel and chromium, preventing the formation of a stable built-up edge. Damage progresses slowly through purely mechanical abrasive wear.

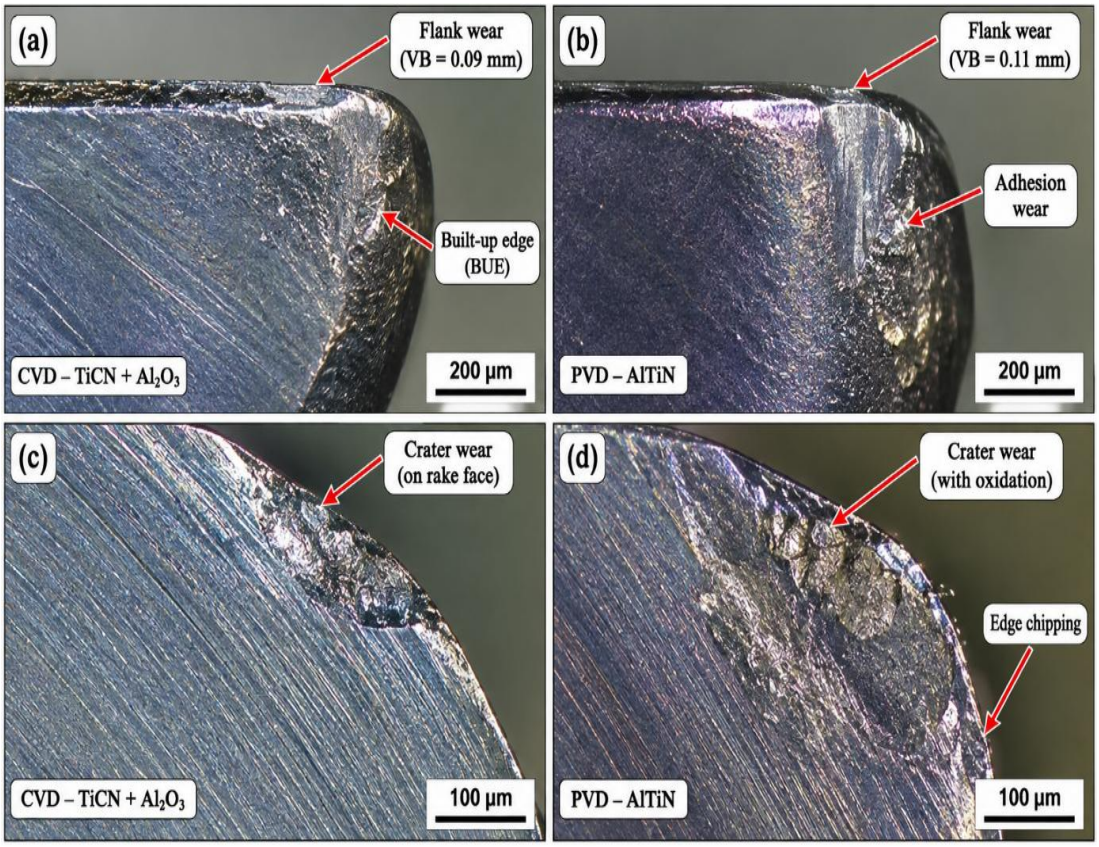


Figure 5 Comparative microscopic morphology of CVD and PVD-coated tungsten carbide cutting tools after 10 min of machining 12X18H10T steel : a) and c) CVD-coated carbide tool (TiCN + Al_2O_3), showing flank wear, built-up edge formation, and crater wear. b), d) PVD-coated carbide tool (AlTiN), showing flank wear, adhesive wear, crater formation with oxidation, and localized chipping of the cutting edge.

4. Conclusions

This comparative study of the performance of PVD and CVD coated tools in terms of tool life, cutting forces, interface temperature and wear, carried out during the turning of 12X18H10T austenitic steel in a dry environment, leads to the following conclusions:

1. From a thermal perspective, for continuous high-speed turning operations ($V = 140m/\text{min}$), the CVD (TiCN+Al_2O_3) coating offers a 35% longer service life (14 minutes of stationary cutting versus 10 minutes for PVD) before reaching the critical failure point ($V_B = 0{,}3\ mm$). Its alumina (α-Al_2O_3) layer, obtained by CVD, provides an essential insulating barrier against the low thermal conductivity of the machined 12X18H10T steel. It effectively protects the carbide substrate against plastic deformation and thermal softening.
2. The chemical inertness of CVD alumina ceramic eliminates the affinity for nickel and chromium in the austenitic matrix, thus preventing the cyclic peeling wear observed

with PVD. The hard TiCN underlayer, meanwhile, offers resistance to micro-abrasion due to the hard titanium carbide (TiC) inclusions characteristic of this steel. The PVD (AlTiN) coating offers superior performance during the initial machining stages thanks to its sharp edge, which limits work hardening of the workpiece surface. It remains highly recommended for finishing, threading, or interrupted machining (milling) operations where cyclic mechanical shocks preclude the use of brittle CVD coatings.

3. Optical microscopy of images taken at different time intervals on the worn tool revealed that adhesion, abrasion, and oxidation were the primary wear mechanisms for both types of tools. A spalling phenomenon on the main cutting edge and strong local welds on the tool surface were also identified as contributing factors to wear in the case of PVD-coated tools. The CVD-coated tool with the Al_2O_3/TiCN coating was protected from thermomechanical stresses, thus preserving the geometry of the cutting edge.
4. Perspectives: The future optimization of the machining of 12X18H10T steels and high-strength steels lies in the development of multilayer nanostructured coatings combining the fineness and compressive stresses of PVD with the chemical inertness of the alumina phases of CVD, which would allow for exceptional wear resistance of carbide cutting tools and improve the cutting performance of PVD and CVD coated tools when machining difficult-to-machine steels.

Author Contributions: G.A.Z.N.: Methodology, investigation, data curation, writing-original draft. J.L.T.: Methodology, investigation, data curation, writing-review and editing, supervision. All authors have read and agreed to the published version of the manuscript.

Funding: The authors extend their appreciation to Volgograd State Technical University for funding this research through grant no. 429 dated 31.08.2023.

Institutional Review Board Statement: Not applicable.

Informed Consent Statement: Not applicable.

Data Availability Statement: Data are contained within the article.

Conflicts of Interest: The authors declare no conflicts of interest.

References

1. Talantov NV (1984) Physical principles of cutting process. In: Physical processes in metal cutting: collection of scientific works (in Russian). Volgograd Polytechnic Institute Publishing House, Volgograd, p 179
2. Talantov NV (1992) Physical principles of the process of cutting, wear and destruction of the tool (in Russian). Mashinostroenie, Moscow
3. Tatar K, Svenningsson I (2026) Investigation of sustainable face milling of austenitic stainless steel: material removal performance and tool modification. Int J Adv Manuf Technol 142:349–359. https://doi.org/10.1007/s00170-025-17010-8

4. Zebaze GNA, Chigirinsky YuL (2025) Modeling of surface quality parameters as a result of machining (in Russian). Izv Volgogr Gos Tekh Univ 1(296):53–56. doi.org
5. Zebaze NGA, Tchigirinsky JuL (2025) Optimization of cutting parameters during CNC turning of a steel. Int J Innov Sci Res Technol 9(12):2610–2615. doi.org
6. Tchigirinsky JuL, Zebaze NGA, Chigirinskaya NV, Norchenko PA, Demchenko IK (2025) Statistical modeling of surface roughness with finish turning of carbon steel (in Russian). Sovrem Naukoemkie Tekhnol 4:90–96. https://doi.org/10.17513/snt.40370
7. Tchigirinsky JL, Trung PH, Lipatov AA (2016) Features of processing of corrosion resistant steels. Mater Sci Forum 870:598–602. doi.org
8. Lipatov AA, Chigirinsky YuL, Kormilitsin SI (2012) Temperature-force characteristics of contact interaction on the wear area of the tool flank surface during turning of austenitic steel (in Russian). Metalloobrabotka 2:38–42
9. Lipatov AA (2013) Features of the transition from build-up formation to interaction with plastic contact during processing of austenitic steel (in Russian). Izv Volgogr Gos Tekh Univ 7(110):31–34
10. Fernández-Abia AI, Barreiro J, López de Lacalle LN et al (2012) Behavior of austenitic stainless steels at high speed turning using specific force coefficients. Int J Adv Manuf Technol 62:505–515. https://doi.org/10.1007/s00170-011-3846-9
11. Dureja JS, Singh R, Bhatti MS (2014) Optimizing flank wear and surface roughness during hard turning of AISI D3 steel by Taguchi and RSM methods. Prod Manuf Res 2(1):767–783. https://doi.org/10.1080/21693277.2014.955216
12. Martinho RP, Silva FJG, Martins C, Lopes H (2019) Comparative study of PVD and CVD cutting tools performance in milling of duplex stainless steel. Int J Adv Manuf Technol 102:2423–2439. https://doi.org/10.1007/s00170-019-03351-8
13. Yasar SA, Uzun G, Korkut I (2026) Experimental evaluation of different coated cutting tools effects on machinability in turning of 17-4 PH stainless steel and optimization of the cutting parameters. Proc Inst Mech Eng Part E J Process Mech Eng 240(3):3318–3327. https://doi.org/10.1177/09544089241285325
14. Sousa VFC, Silva FJG (2020) Recent advances in turning processes using coated tools - a comprehensive review. Metals 10(2):170. https://doi.org/10.3390/met10020170
15. Gislain Anicet ZN, Tchigirinsky JL (2026) Phase transformations in carbon steels and their influence on machining during heat treatment. Int J Adv Manuf Technol 146:327–334. https://doi.org/10.1007/s00170-026-18822-y
16. Zebaze NZhA, Tchigirinsky JuL, Moiseev DV (2026) Modification the thermophysical and mechanical properties of steels during machining (in Russian). Izv Volgogr Gos Tekh Univ 1(308):27–32. doi.org
17. Zebaze NZhA, Tchigirinsky JuL (2026) Construction and analysis of the Fe-C phase equilibrium diagram for corrosion–resistant steels (in Russian). Izv Volgogr Gos Tekh Univ 3(310):21–26. doi.org
18. Vitoussia T, Brillard A, Bertsch J et al (2021) Analysis and modeling of the thermal behavior of an improved pellet cookstove. SN Appl Sci 3:652. https://doi.org/10.1007/s42452-021-04630-4